



A MICROCONTROLLER BASED LED SUNPHOTOMETER WITH RF DATA ACQUISITION

Cesar A. Llorente¹, Benison S. Ongsyng¹, Paolo Gabriel P. Casas¹, Matthew Lewis C. Chan¹,
Glenn Michael San Pedro¹, Edgar A. Vallar² and Maria Cecilia D. Galvez²

¹Department of Electronics and Communications Engineering

²Environment And RemoTe sensing researchH (EARTH) Laboratory, Department of Physics
De La Salle University, Taft Avenue, Malate, Manila, Philippines

E-Mail: cesar.llorente@dlsu.edu.ph

ABSTRACT

A microcontroller based four-channel LED sunphotometer system with RF transceiver system was successfully developed in this study. The control and data acquisition was done wirelessly using a Zigbee RF Transceiver Module. The RF transceiver module was connected to the sun tracking mount and to a personal computer. Sun tracking was done using a quadrant photodiode for feedback control and a mathematical algorithm for tracking the sun for low-sunlight intensity situations. High correlation coefficients were obtained when the data obtained from the four LED channels of the system was compared with a commercial four channel SP02 sunphotometer. With this system, the sun tracking mount can be placed anywhere without the need for long wires as long as there exists a line of sight between the two RF transceiver modules.

Keywords: LED, sunphotometer, microcontroller, radio frequency, aerosol.

INTRODUCTION

The concept of sunphotometry started with Volz in 1974 (Volz, 1974). It is a passive remote sensing technique using the Sun as the light source. As sunlight enters the atmosphere, its intensity is reduced by aerosol absorption and scattering. A sunphotometer is a device that measures the intensity of the sunlight as it reaches the earth and this can give information on the amount of aerosols in the atmosphere. Knowledge on the amount and optical properties of aerosols are very important as aerosols have direct and indirect effects on the earth's energy budget and climate change. In 1992, Mims first described a light emitting diode (LED) based sunphotometer (Mims, 1992). This is a low-cost sunphotometer which uses LEDs as a detector and also as interference filters. This kind of sunphotometer has been used in global aerosol monitoring networks such as the Global Learning and Observations to Benefit the Environment (GLOBE) program (Mims, 1999). The GLOBE network used a two channel handheld LED sunphotometer. Since then several innovations were made with this kind of photometer such as in increasing the number of LEDs and in various ways of acquiring the data (Huang *et al.*, 1998; Mousazadeh *et al.*, 2009; Hewitson, 2007; Robles, 2000; Macalalad, 2004; Macalalad, 2006). Since most LED sunphotometers were either handheld or used long wires to control and acquire data, in this paper, we will present a four channel LED sunphotometer that used a microcontroller to automate the sun tracking mechanism and data transmission with a wireless control system using transceiver modules connected to the sun tracking mount and to a PC/laptop. With this system, the

sun tracking mount can be placed anywhere without the need for long wires as long as there exists a line of sight between the two RF transceiver modules.

THE LED SUNPHOTOMETER SYSTEM

The LED sunphotometer system constructed in this study includes an optical sensor box, the sun tracking mount, the microcontroller, and the Zigbee RF Transceiver Module. This section describes each component of the system.

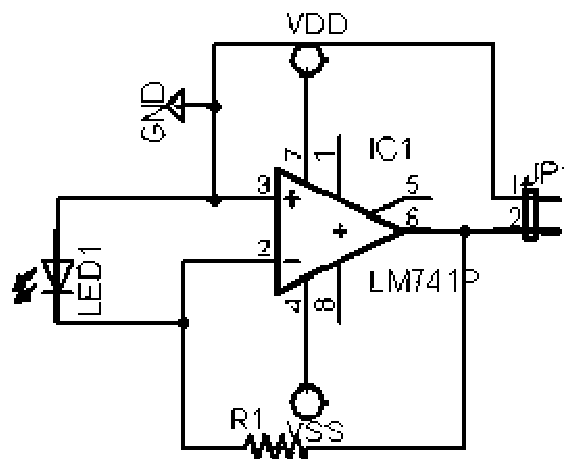


Figure-1. Schematic diagram of LED sensor circuit.



The optical sensor

The optical sensor box contains the four lamp type LEDs (blue, green, red, and orange) that were used as a detector. An LED when exposed to light (of the correct frequency range) produces a photo current. This current is a measure of the intensity of the light to which it is exposed to. The signal from the LEDs will go through LM741 (National Semiconductor, 2000) op-amps to be amplified, enough for the microcontroller to read it. The gain can be controlled by adjusting the feedback resistor from the circuit shown in Figure-1. The amplified signals will go through an analog-to-digital converter in the development board. The signals will then be sent to the computer via the transceivers.

Also included in the optical sensor box is the quadrant photodiode. The quadrant photodiode (QPD) selected for the study was the QP50-6SD2 (Pacific Silicon Sensor Inc., 2009). It is a quadrant photodiode array with current-to-voltage amplifiers that provide bottom minus top (B-T) and left minus right (L-R) difference signals. It also includes a sum signal that provides the sum of all four quadrant signals. The difference signals are analog voltage outputs of the light intensity difference sensed by the pairs of photodiode elements in the array. The device features a 7 pin connector for easy hook up. It acts as a feedback system for locating the position of the sun. The quadrant photodiode operates by locating the position of the sunlight from the pinhole of the optical sensor box. It uses the bottom minus top (B-T) and left minus right (L-R) difference signals to pinpoint in which quadrant is the spot of the sun located. The data is sent to the microcontroller, and the microcontroller computes the adjustments to the altitude and azimuth motors so that the sun's spot will be centered in the origin of the QPD. The microcontroller then sends signals to the motors to move the position of the sun photometer. The encoders will detect if the motors have moved accordingly. The encoders signal the microcontroller of the motor status, and let the microcontroller decide if it is satisfied with the position of the sun photometer.

The sun tracking mount

The sun tracking mount consists of the top, middle, and lower section. The top section shown in Figure-2 contains the optical sensor box, the gearbox, the altitude motor, and the encoder. This section handles the altitude positions of the sun. The sensor box features an adjustable pinhole for a more convenient method of centering the quadrant photodiode. A set of bearings underneath allows the frame to rotate freely at the same time support its entire weight. The middle section, shown in Figure-3, contains a stepper motor, a gearbox, an encoder and some rotational parts necessary for the azimuth adjustment. The stepper motor used in this section is slightly more powerful than that of the upper section to accommodate everything above. The bottom section is the

base of the sunphotometer. It contains the humidity sensor, microcontroller and power supply. Basically, it acts as the hub of the entire device. The transceiver was connected externally via an extension cable to maximize signal reception.

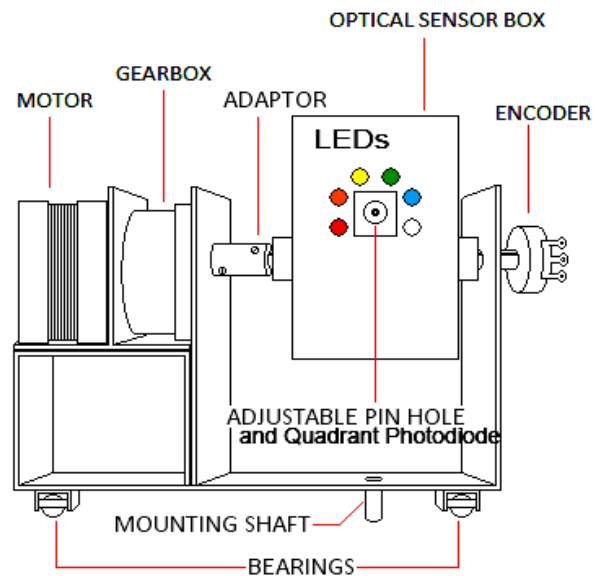


Figure-2. Top section of the sun tracking mount.

The stepper motors

The azimuth stepper motor used was the 4023-819 unipolar stepper motor. It features a 53 oz-in minimum holding torque, 1.8 degree step and a rotational inertia of 100 g-cm². It operates at a 5.1V 1A rating. It was programmed to move at half step intervals for better accuracy. These NEMA standard 2 phase 1.8 degrees hybrid step motors offer high torque in a compact lightweight rugged housing. A variety of windings are available to meet most application requirements. These motors offer fast damping and high slew rates for better control in full/half or micro step mode. The torque levels reached with this step motor line makes them a cost effective alternative to servo motors in many applications. For the altitude motor, we used a smaller but still powerful motor, kh42hm28058. This motor has a step size of 1.8 degrees, high torque but low in noise and vibration, suitable for the tracking of the sun. Its special features include improved dynamic torque, lowered vibration and noise level. Lastly, it has improved efficiency by using high grade materials.

The gearbox

The gearbox used was based on available products in the market. The GS38.0010 gearbox was selected because it had a 10:1 ratio. When attached to the 0.9 degree



half step motor, the output step size was computed to have an accuracy of 0.09 degree per step.

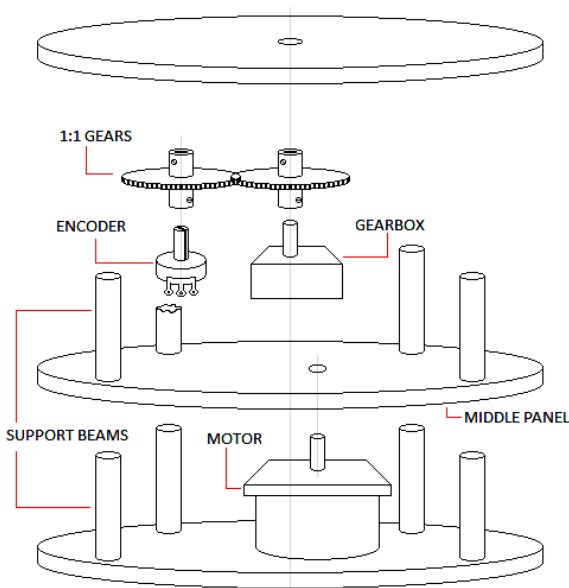


Figure-3. Middle section of the sun tracking mount.
top section of the sun tracking mount.

The encoders

The motor encoders were potentiometers. 1 K Ω potentiometers were chosen so that the device would not consume too much power. It is more economical and flexible than other encoders in the market, because its analog output can be connected to any Analog to Digital Converter (ADC). The system was designed to have an accuracy of 0.09 degrees per step. Dividing this by 360 degrees gives 4000 steps in a full rotation. The number of bits for the ADC was computed to be 12 bits since it will result to 4096 combinations. A gear system with a ratio of 1:1 was placed in the central rotational shaft and the encoder shaft.

The microcontroller

The Microcontroller used in the system was the ARM Cortex M3 32-bit (ARM Ltd., 2015). It provides a high-performance, low-cost platform for a broad range of applications including automotive body systems, industrial control systems and wireless networking, etc. The Cortex-M3 provides outstanding computational performance and exceptional system response to interrupts while meeting low cost requirements and low power consumption. Its major advantages include real time behaviour with minimal interrupt latency and a wide range of operating temperature from -40 to +85°C or up to 105°C. The central core of the Cortex-M3 is based on a 3-stage pipeline and delivers an

efficiency of 1.25 DMIPS/MHz. It can run in C and assembly language. The microcontroller used the STM32F103 Development board which features a 128 KB flash memory, 12-bit analog-to-digital converter, 32-bit microcontroller with real-time clocking, and RS232/USB ports that will allow easy interfacing of the sunphotometer parts (Futurlec, 2015). It uses C language programming, and compiles with the Keil C Compiler, which can be acquired through downloading.

Zigbee RF transceiver module

For the RF transceiver module, we used Zigbee (MaxStream Inc., 2005). It is a low cost and low power wireless technology and has an IEEE standard of 802.15.4 with added network functionality. It operates in the following frequency bands: 2.400-2.484 GHz, 902-928 MHz, and 868.0-868.6 MHz. Some of its features include a long battery life because of having a low duty cycle, capability of supporting various network topologies; can carry up to 65,000 nodes on a network, much tighter security because it implements 128-bit AES encryption and good packet handling capabilities. One of its most important advantages is that it can support mesh networks. This is a key factor because in mesh networks, the nodes are dynamically updated and optimized. With ad-hoc routing, this network can provide greater stability in different node conditions.

DEVICE SYSTEM FLOW OF OPERATION

A representation of the device operation system block diagram is shown in Figure-4. The processes are grouped by colors for easier reference. The optical sensor box will detect the main input for the sun photometer. The LEDs will measure the voltage readings from the sunlight. The signals will be fed to the analog-to-digital converter in the development board. The quadrant photodiode will determine the position of the sun. The signals will go to the microcontroller to be processed. The microcontroller will compute for the number and direction of steps that will center the sun's spot in the quadrant photodiode. It signals the motors to adjust the position of the sun photometer. The procedure for tracking the sun using the feedback system and mathematical algorithm was similar to the one described in Macalalad (2006). The signal goes through driver circuits to drive the motors. As the motors move, the encoders verify the movement.

The humidity sensor protects the sunphotometer against rain. The humidity sensor measures the humidity level. If it reaches a threshold value, it will signal the microcontroller that rain is about to pour. The microcontroller then signals the motors to rotate the optical sensor box facing downwards to prevent rain from entering the exposed holes for the sensors. When the humidity level normalizes again, it will signal the microcontroller to resume tracking the sun's position. The microcontroller transfers the data to the transmitter module



to be sent to the receiving host. When the receiver module receives the data, the data is passed on to the computer. The computer will then translate the data. The data is stored in the computer which also handles all the processes relevant to the study.

RESULTS AND DISCUSSION

To test the LED sunphotometer system developed in this study, experiments were conducted simultaneously with a commercial sunphotometer. The commercial sunphotometer was an SP02 Middleton sunphotometer having 4-channels with center wavelengths at 368, 500, 675, and 862 nm. Detailed information about the DLSU-EARTH SP02 sunphotometer is available in Macalalad (2004). Experiments were conducted at the rooftop of the DLSU Science and Technology Research Center. Figure-5 shows the data acquired for the LED sunphotometer system (represented by the solid line) and the commercial sunphotometer (represented by the dot markers).

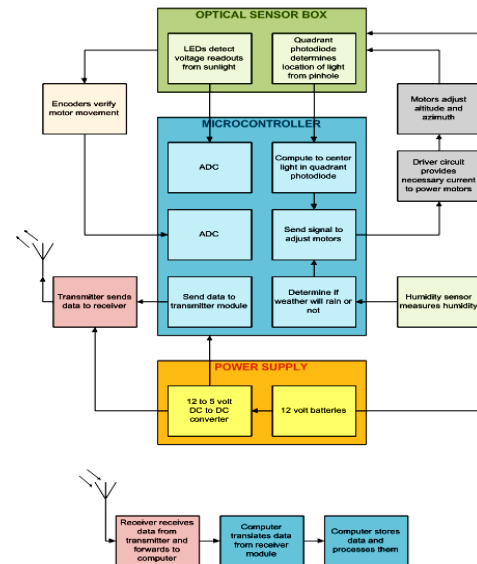
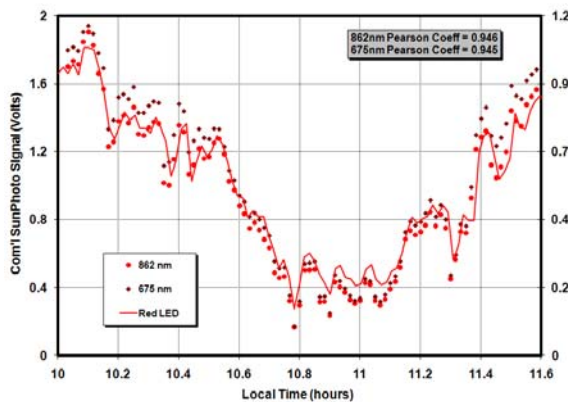
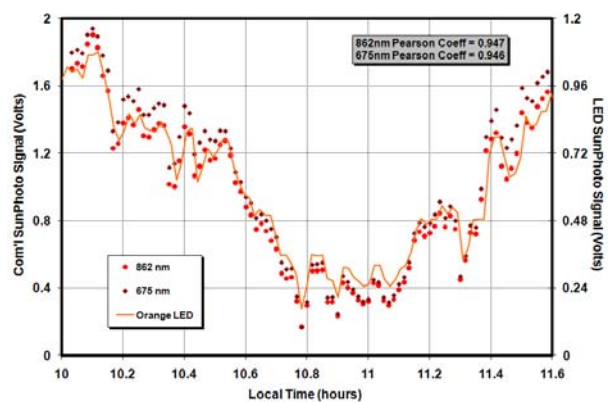


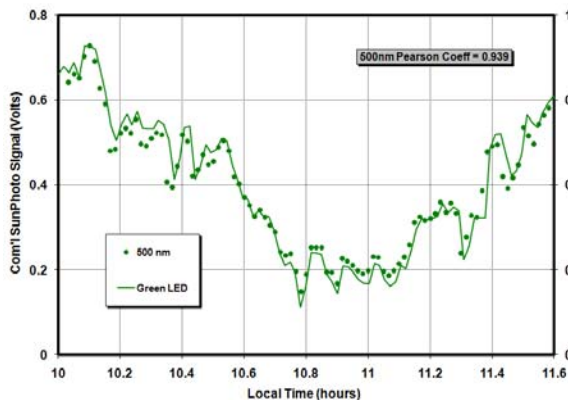
Figure-4. System block diagram of the sunphotometer.



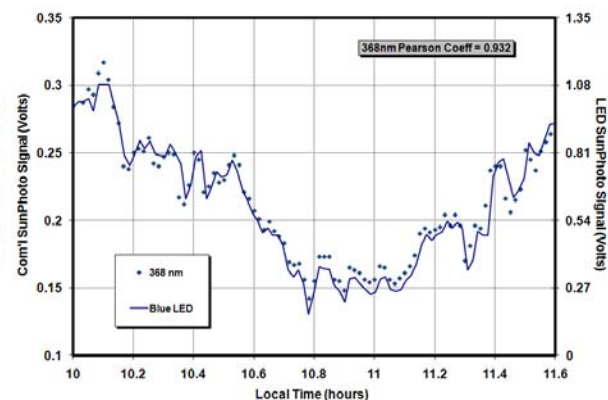
(a) Red LED, 675 nm, and 862 nm signal voltage.



(b) Orange LED, 675 nm, and 862 nm signal voltage.



(c) Green LED and 500 nm signal voltage



(d) Blue LED and 368 nm signal voltage

Figure-5. Signal voltage from LED and SP02 sunphotometers.



The data from the red and orange LED was compared with the 675 and 862 nm channels of the commercial sunphotometer, whereas the green LED and the blue LED were compared with the 500 nm and 368 nm channels, respectively. As can be seen from Figure-5, the trends of the voltages from both sunphotometers are the same. Pearson correlation coefficient was used to check how the signal voltages from both sunphotometers correlate with one another. Figure-6 shows the linear fit between the commercial and the LED Sunphotometer while Table-1 summarizes the Pearson coefficient obtained using MS Excel. The Pearson coefficient obtained from all the channels were all greater than 93% indicating that the signal behaviour from the LED sunphotometer system developed in this study is comparable to the commercial sunphotometer. It means that the wireless control and data acquisition were working properly.

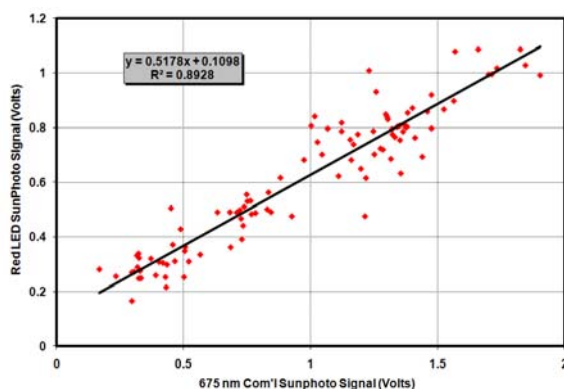
CONCLUSIONS

A microcontroller based four-channel LED sunphotometer system with RF transceiver system was successfully developed in this study. The control and data acquisition was done wirelessly using a Zigbee RF

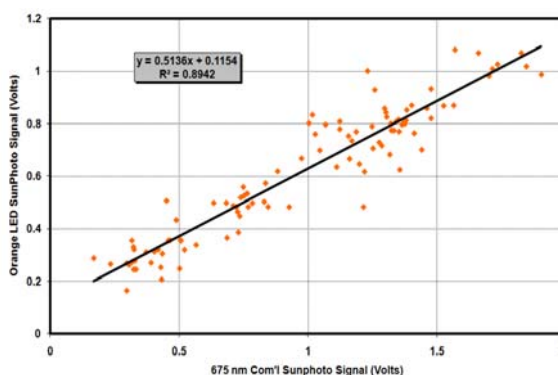
Transceiver Module. The RF transceiver module was connected to the sun tracking mount and to a portable PC. Sun tracking was done using a feedback control in combination with a mathematical algorithm for tracking the sun during low sunlight intensity situations. A quadrant photodiode was employed for the feedback control. High correlation coefficients were obtained as the data gathered from the four LED channels of the system was compared with a commercial four channel SP02 sunphotometer. With this system, the sun tracking mount can be placed anywhere without the need for long wires as long as there exist a line of sight between the two RF transceiver modules.

Table-1. Computed Pearson's coefficient.

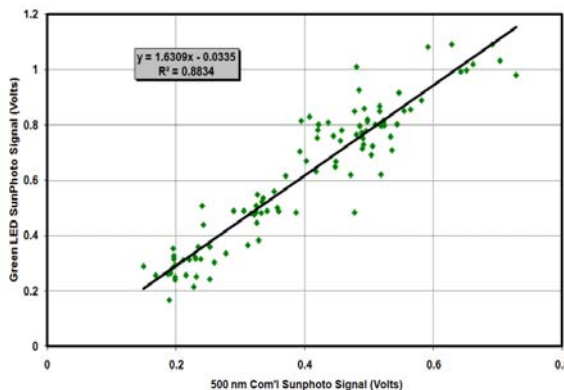
Color	Pearson's coefficient (r)
Red vs. 675nm Red	0.945
Orange vs. 675nm Red	0.946
Green vs. 500nm Green	0.940
Blue vs. 368nm Blue	0.932



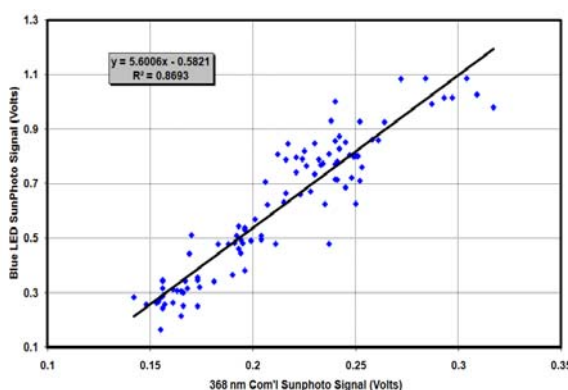
(a) Red LED and 675 nm signal voltage.



(b) Orange LED and 675 nm signal voltage.



(c) Green LED and 500 nm signal voltage



(d) Blue LED and 368 nm signal voltage

Figure-6. Correlation between LED and SP02 sunphotometers.



REFERENCES

ARM Ltd. 2015. Cortex-M3 Processor. Retrieved August 10, 2015 from <http://www.arm.com/products/processors/cortex-m/cortex-m3.php>.

Futurlec. 2015. STM32F103 Development Board. Retrieved August 22, 2015 from http://www.futurlec.com/STM32_Development_Board.shtml.

Hewitson J. 2007. Design of a micro processor based automated Sun photometer. Undergraduate Thesis, Faculty of Engineering, Department of Electrical Engineering, University of Cape Town, USA.

Huang F, Tien D, Or J. 1998. A Microcontroller Based Automatic Sun Tracker Combined with a New Solar Energy Conversion Unit. Power Electronic Drives and Energy Systems for Industrial Growth, Proceedings. 1998 International Conference. (1): 488-492.

Macalalad E. 2004. Retrieval of Multi-spectral Aerosol Optical Depth (AOD) and Development of a Sun Tracking Device for the SP101 and SP02 Sunphotometers. Undergraduate Thesis, Physics Department, De La Salle University, Manila, Philippines.

Macalalad E. 2006. Determination of Atmospheric Turbidity Parameters and Aerosol Size Distribution Using a Feedback-Controlled Sun Tracking Sunphotometer over Manila. Master Thesis. Physics Department, De La Salle University, Manila, Philippines.

MaxStrem Inc. 2005. XBee OEM RF Modules. Retrieved October 16, 2010 from <http://www.reved.co.uk/docs/xbe001.pdf>.

Mims III, F. M. 1992. Sun Photometer with Light-Emitting Diodes as spectrally selective detectors. Appl. Opt. 31, 6965-6967.

Mims III, F.M. 1999. An international haze-monitoring network for students, Bulletin of the American Meteorological Society. 80, 1421-1431.

Mousazadeh H, Keyhani A, Javadi A, Mobli H, Abrinia K, Sharifi A. 2009. A review of principle and sun-tracking methods for solar systems output. Renewable and Sustainable Energy Reviews. 13(8): 1800-1818.

National Semiconductor. 2000. LM741 Operational Amplifier. Retrieved October 16, 2010 from <http://www.national.com/ds/LM/LM741.pdf>.

Pacific Silicon Sensor Inc. 2009. Quad Sum and Difference Amplifier. Retrieved October 16, 2010 from <http://www.pacific-sensor.com/pdf/QP506SD2.pdf>.

Robles I. M. A. 2000. Construction of an LED-Sensored Sunphotometer and Measurement of the Atmospheric Optical Thickness, Undergraduate Thesis, Physics Department, De La Salle University, Manila, Philippines.

Volz F.E. 1974. Economical multispectral Sun photometer for measurements of aerosol extinction from 0.44mm to 1.6 mm and precipitable water. Appl. Opt. 13, 1421-1431.